Spectral Signatures of L-DOPA-Induced Dyskinesia Depend on L-DOPA Dose and are Suppressed by Ketamine

Tony Ye[1], Mitchell J. Bartlett[1, 2], Scott J. Sherman[1], Torsten Falk[1, 2], Stephen L. Cowen[3*]

1 Department of Neurology, University of Arizona College of Medicine, Tucson, AZ, United States
2 Department of Pharmacology, University of Arizona College of Medicine, Tucson, AZ, United States
3 Department of Psychology, University of Arizona, Tucson, AZ, United States

*** Correspondence:**

Stephen L Cowen scowen@email.arizona.edu

Authors and Affiliations:

Tony Ye tye@ucla.edu
- Department of Neurology, University of Arizona College of Medicine, Tucson, AZ, United States
- Work was completed at the University of Arizona, but present address is UC Los Angeles.

Mitchell J Bartlett mbartlet@email.arizona.edu
- Department of Neurology, University of Arizona College of Medicine, Tucson, AZ, United States
- Department of Pharmacology, University of Arizona College of Medicine, Tucson, AZ, United States

Scott Sherman ssherman@neurology.arizona.edu
- Department of Neurology, University of Arizona College of Medicine, Tucson, AZ, United States

Torsten Falk tfalk@arizona.edu
- Department of Neurology, University of Arizona College of Medicine, Tucson, AZ, United States
- Department of Pharmacology, University of Arizona College of Medicine, Tucson, AZ, United States

Stephen L Cowen scowen@email.arizona.edu
- Department of Psychology, University of Arizona, Tucson, AZ, United States

Keywords: levodopa-induced dyskinesia; Parkinson's disease; oscillation; gamma; high-frequency oscillation; cross-frequency coupling; ketamine

Running Title: Spectral Signatures of Dyskinesia and Ketamine

Word Count: 5916 **Abstract Word Count:** 372

Number of Figures: 8 **Supplements:** 5 Figures, 1 Table

Abstract

L-DOPA-induced dyskinesias (LID) are debilitating motor symptoms of dopamine-replacement therapy for Parkinson's disease (PD) that emerge after years of L-DOPA treatment. While there is an abundance of research into the cellular and synaptic origins of LID, less is known about how LID impacts systems-level circuits and neural synchrony, how synchrony is affected by the dose and duration of L-DOPA exposure, or how potential novel treatments for LID, such as sub-anesthetic ketamine, alter this activity. Sub-anesthetic ketamine treatments have recently been shown to reduce LID, and ketamine is known to affect neural synchrony. To investigate these questions, we measured locomotor and local-field potential (LFP) activity from the motor cortex (M1) and the striatum of preclinical rodent models of PD and LID. In the first experiment, we investigated the effect of the LID priming procedures and L-DOPA dose on neural signatures of LID. Two common priming procedures were compared: a high-dose procedure that exposed unilateral 6-hydroxydopamine-lesioned rats to 12 mg/kg L-DOPA for 7 days, and a low-dose procedure that exposed rats to 7 mg/kg L-DOPA for 21 days. Consistent with reports from other groups, high-dose priming triggered LID and 80-Hz oscillations; however, these 80-Hz oscillations were not observed under the low-dose procedure despite clear evidence of LID, indicating that 80-Hz oscillations are not an exclusive signature of LID. Instead, the low-dose procedure resulted in the weeks-long gradual emergence of non-oscillatory broadband gamma activity (> 30 Hz) in the striatum and theta-to-high-gamma cross-frequency coupling (CFC) in M1. In a second set of experiments, we investigated how ketamine exposure affects spectral signatures of low-dose L-DOPA priming. During each neural recording session, ketamine was delivered through 5 injections (20 mg/kg, *i.p.*) administered every 2 hours. We found that ketamine exposure suppressed striatal broadband gamma associated with LID, but enhanced M1 broadband activity. We also found that M1 theta-to-high-gamma CFC associated with the LID on-state was suppressed by ketamine. These results suggest that ketamine's therapeutic effects are region specific. Our findings also have clinical implications as we are the first to report novel oscillatory signatures associated with the common low-dose LID priming procedure that more closely models dopamine replacement therapy in individuals with PD, and as we identify neural correlates of the anti-dyskinetic activity of sub-anesthetic ketamine treatment.

Introduction

Parkinson's disease (PD) is a neurodegenerative disease with cardinal motor impairments of bradykinesia, rigidity, postural instability, and tremor (Olanow et al., 2009). These motor dysfunctions are caused by the death of dopaminergic neurons in the substantia nigra pars compacta (SNc) that project to the striatum, resulting in reduced dopaminergic tone in corticostriatal circuits. The gold-standard treatment for PD is dopamine replacement therapy via the dopamine precursor L-3,4-dihydroxyphenylalanine (L-DOPA). L-DOPA restores physiological dopamine concentrations in the striatum (Picconi et al., 2003) to reinstate voluntary motor activity. However, prolonged L-DOPA exposure eventually leads to incapacitating L-DOPA-induced dyskinesias (LID) (Cotzias et al., 1969), making untenable continued L-DOPA treatment. Consequently, new approaches are needed for treating LID and extending L-DOPA's window of clinical efficacy.

The changes associated with LID are believed to alter circuits in the basal ganglia and motor cortex (M1), and these alterations result in beta (~20 Hz) and high-gamma (~80 Hz) band neural oscillations (Litvak et al., 2011). For example, clinical studies have identified an 80-Hz signature of LID in the subthalamic nucleus (STN) in human patients (Alonso-Frech et al., 2006; Lopez-Azcarate et al., 2010). To investigate LID-associated gamma oscillations in preclinical rodent models, several groups utilized a 7-d L-DOPA priming protocol (12 mg/kg) in 6-hydroxydopamine-(6-OHDA) lesioned animals, and they found that L-DOPA induces a narrow-band 80 Hz gamma oscillation in M1. This 80-Hz oscillation is sometimes referred to as "finely-tuned gamma", and is associated with abnormal involuntary movements (AIMs) produced by L-DOPA (Dupre et al., 2016; Halje et al., 2012). These observations suggest that treatments that reduce striatal 80-Hz gamma could also reduce LID symptoms.

It is not known whether cortical narrow-band 80-Hz oscillations are common in human patients or in preclinical models of LID. Only one investigation in human subjects has been performed that shows clear 80-Hz activity in the STN (Williams et al., 2002). Furthermore, studies of oscillatory activity using preclinical models of LID utilize multiple priming protocols (Bartlett et al., 2016; Cenci et al., 1998; Dekundy et al., 2007; Dupre et al., 2016; Halje et al., 2012). Consequently, it is possible that some of the identified oscillatory signatures of LID are unique to the dosage and duration of L-DOPA exposure. Broadly, LID priming procedures can be divided into low-dose+long-duration (*e.g.*, 7 mg/kg for 21 d; Cenci *et al.*, 1998; Dekundy *et al.*, 2007;

Bartlett *et al.*, 2016) and high-dose+short-duration protocols (*e.g.*, 12 mg/kg, 7-d; Halje *et al.*, 2012*b*; Dupre *et al.*, 2016). There are clear advantages to both procedures. For example, the high-dose priming produces results in the LID behavioral phenotype on the first day of exposure, which can be of significant practical advantage (Carta et al., 2006). In contrast, low-dose (7 mg/kg) 21-d priming produces more gradual development of LID that better reflects development of LID in patients. No study to date has investigated the influence of the priming protocol on oscillatory signatures of LID. Determining whether LID-associated oscillations are impacted by the dosage or duration of L-DOPA administration is important given the variety of clinical dosages of L-DOPA given to PD patients.

Low-dose sub-anesthetic ketamine has been successfully used to treat chronic pain (Niesters et al., 2014) and treatment-resistant depression (Andrade, 2017; Diamond et al., 2014), with *S*-ketamine now being an FDA approved drug for use in treatment-resistant depression (Kaufman, 2019). A retrospective case study in PD patients receiving sub-anesthetic infusions of ketamine to treat pain showed reduced LID for up to one month (Sherman et al., 2016). In a rodent LID model, sub-anesthetic ketamine treatment can reduce LID long-term (Bartlett et al., 2016). These lasting effects may be due to ketamine's ability to modify oscillatory activity throughout the brain (Hunt and Kasicki, 2013; Ye *et al.*, 2018). A single injection of sub-anesthetic ketamine is known to trigger oscillatory activity throughout corticostriatal and hippocampal circuits (Caixeta et al., 2013; Nicolás et al., 2011; Olszewski et al., 2013). In addition, we have shown in naïve rats that repeated sub-anesthetic injections trigger region-wide and dose-dependent high-frequency oscillations (HFO, >100 Hz), broadband asynchronous gamma (40–80 Hz), and cross-frequency interactions (Ye et al., 2018).

In this study, we investigated whether the LID-induction protocol or the L-DOPA dose administered during LID induction resulted in unique oscillatory signatures. We also investigated the hypothesis that ketamine produces its anti-dyskinetic effect by suppressing neural oscillations associated with LID. These questions were investigated through the measurement of local-field activity in M1, dorsolateral striatum (DLS), dorsomedial striatum (DMS), and the nucleus accumbens (NAc) in awake and behaving unilateral 6-OHDA-lesioned rats treated with L-DOPA.

Materials and Methods

Animals:

Twenty-seven male Sprague-Dawley rats (6 weeks old, 250-275 g at arrival, Harlan Laboratories, Indianapolis, IN) were single-housed in a temperature and humidity controlled 12-hr reverse light/dark cycle room with food and water available *ad libitum*. Rats were divided into four groups based on lesion or L-DOPA treatment: naïve non-lesioned controls (n=8), PD (n=7), LID 7-d priming (n=6), and LID 21-d priming (n=7). Sample sizes for groups were determined by previous experiments (Ye et al., 2018). All procedures were in accordance with NIH guidelines for the Care and Use of Laboratory Animals and approved IACUC protocols at the University of Arizona.

Unilateral 6-OHDA-lesion PD model:

As previously published (Bartlett et al., 2016), 6-OHDA hydrochloride was injected into 2 locations (5 μg/site) of the medial forebrain bundle. Amphetamine-induced (5.0 mg/kg, *i.p.,* Sigma-Aldrich) rotations were scored by blinded experimenters to assess degree of lesion (**Fig. 1F**). An average score ≥5 corresponds to >90% dopamine depletion (Dekundy et al., 2007). Rats that reached criteria were divided into three groups: LID induction with 7-d priming (n=6), 21-d priming (n=7), or PD (n=7).

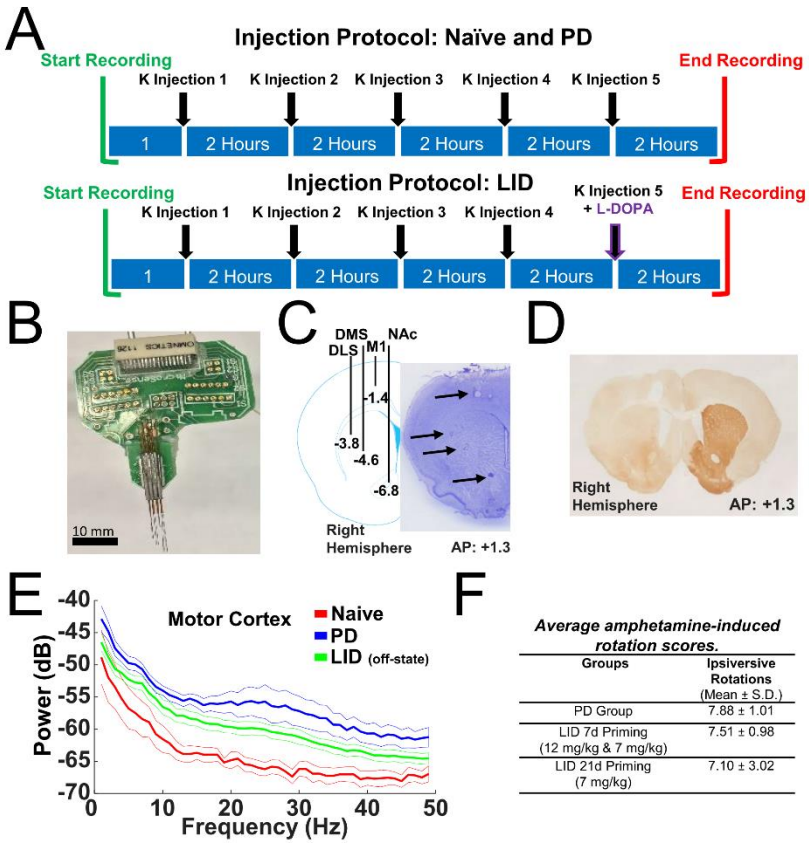

Figure 1. Experimental design and neural recordings. (A) TOP: Timeline of a single experimental session for naïve and 6-OHDA-lesioned animals. Each session began with one hour of pre-injection baseline. At the 2nd hour, a single injection of sub-anesthetic ketamine (20 mg/kg, i.p.) or saline was administered and repeated every 2 hours for a total of 5 injections across each 11+hour session. BOTTOM: Timeline of a single experimental session for animals with L-DOPA-induced dyskinesia (LID). This experimental protocol is identical to the naïve/6-OHDA groups except for a co-injection of L-DOPA (7 mg/kg, i.p.) with ketamine on the 5th injection. Each animal received a single ketamine or saline injection recording session each week. (B) A custom-made 32-channel electrode surgically implanted into the right hemisphere of all experimental animals. (C) Schematic of electrode array placement (AP: +1.3, ML: +2.7 centered, DV: -6.8 deepest electrode) and representative example of histological verification of targets. RIGHT: Verification of 6-OHDA lesioning in 6-OHDA and LID animals via tyrosine-hydroxylase staining. Expression of tyrosine-hydroxylase (dark pigmentation; left hemisphere) is a marker of functioning dopaminergic neurons. (D) Verification of a successful (>90%) 6-OHDA lesion results in a light pigmentation of the striatum (right hemisphere). (E) Average baseline power (Mean ± SEM) of Naïve, PD, and LID (off drug) animals. Mean ± SEM. (F) Average (Mean ± S.D.) cumulative amphetamine-induced rotations and Abnormal Involuntary Movements Scale (AIMs) for PD and LID animals.

Electrode implantation:

Following the procedure reported in Ye *et al.*, 2018, rats were anesthetized with isoflurane and implanted with two custom-made 32-channel electrode arrays, with each array composed of 16 twisted-wire stereotrodes (California Fine Wire Co., Grover Beach, CA). All recordings were referenced to a cerebellar skull screw. The anterior array was placed in the right hemisphere, and individual stereotrodes targeted M1 (AP:+1.3, ML:+2.3, DV:-1.4), DLS (AP:+1.3, ML:+3.5, DV:-

3.8), DMS (AP:+1.3, ML:+2.9, DV:-4.6), and NAc (AP:+1.3, ML:+1.7, DV:-6.8) (**Fig. 1C**). The posterior array was implanted over the hippocampus (centered at AP: −3.0, ML: +2.2) with electrodes lowered near the fissure (DV: −3.2), CA1 (DV: −2.3), dentate gyrus (DV: −3.8), and S1 (DV: −1.4). Rodent welfare was monitored daily by experimenters and animal care staff. Post-operative analgesia: 5 mg/kg (s.c.) Carprofen (Zoetis, Parsippany, NJ) for 48 h post-surgery. Topical anti-biotic ointment (Water-Jel Technologies, Carlstadt, NJ) given for up to 5 days as needed. The non-lesioned naïve control rats were surgically implanted 2-3 weeks after arrival (~4 months old). The PD and LID 7 d priming groups were implanted approximately one week after amphetamine rotation tests (~5 months old), and the LID 21 d priming group were implanted after the 21-d priming period (~6 months old).

Drug treatments:

Using a paradigm described in Bartlett and colleagues (2016), drugs were delivered during neural recording sessions through five intraperitoneal (*i.p.*) injections of ketamine or saline (**Fig. 1A**). The first injection was delivered (6 AM) after one hour of baseline recording. Each injection was separated by two hours. Injections were either ketamine hydrochloride (20 mg/kg) (Clipper Distributing, St. Joseph, MO) or 0.9% saline (SAL) solution. For the LID rats, the 5th injection of ketamine or SAL included a co-injection of L-DOPA (7 mg/kg, *i.p.*, Sigma-Aldrich).

7-d and 21-d LID priming in 6-OHDA-lesioned rats, maintenance, and behavioral analysis:

Rats in the high-dose 7-d L-DOPA priming group (*n*=6) were treated daily with L-DOPA (12 mg/kg) + benserazide (15 mg/kg, *s.c.*, Sigma-Aldrich) for 7 d (*i.e.*, during L-DOPA priming) (**Fig. 2A**). Rats in the low-dose 21-d L-DOPA priming group were treated daily with L-DOPA (7 mg/kg, *i.p.*.) + benserazide (14 mg/kg) for 3 weeks, as previously published (Bartlett et al., 2016) (**Fig. 2D**). Rats in the 21-d group received maintenance doses of L-DOPA (7 mg/kg + 15 mg/kg benserazide) following the 21-d priming period (two doses per week, every 2-3 days for the remainder of the experiment). L-DOPA-induced AIMs were scored by an experimentally blinded investigator on a scale from 0 to 4 (**Fig. 2G**). After the 21-d priming period, rats that met behavioral criteria (*n*=7) proceeded to surgical implantation. This contrasts with the 7-d priming group that

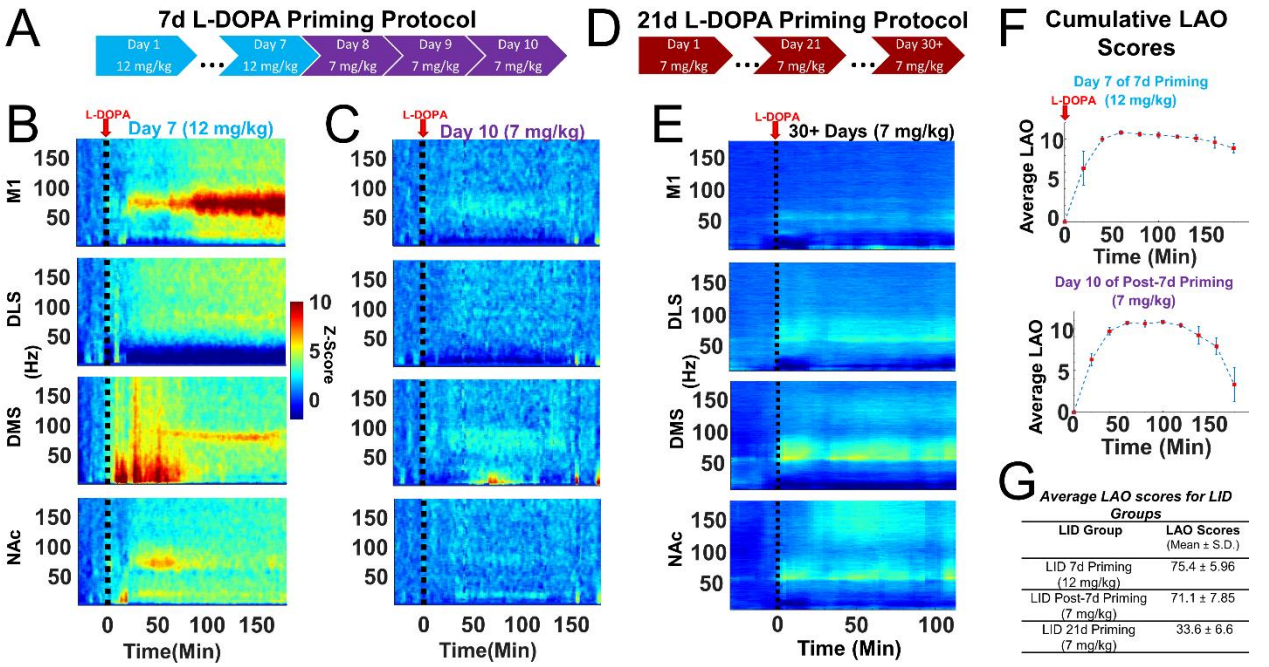

Figure 2. Priming dose- and duration-dependent oscillatory responses of L-DOPA in LID animals. (A) Timeline of 7d L-DOPA priming at 12 mg/kg (blue). After the 7th day, the same animals were treated with 7 mg/kg of L-DOPA (purple). (B) Average spectral power (n=6) of the 7d L-DOPA priming protocol on the 7th day of exposure in motor cortex, dorsolateral- and dorso-medial striatum, and the nucleus accumbens. (n=6). All neural activity was normalized to the pre-injection baseline (-32 to -2 min). (C) As in (left), but for the third exposure to 7 mg/kg of L-DOPA in the same animals. (D) Timeline of 21d L-DOPA priming at 7 mg/kg. Maintenance doses of L-DOPA (7 mg/kg) were administered every 2-3 days after the 21d priming to maintain stable dyskinesia. (E) Average spectral response during L-DOPA (7 mg/kg) after 21d of priming at the same dose (n=7). All neural activity was normalized to the pre-injection baseline (-32 to -2 min). (F) Cumulative Limb, Axial, and Orolingual (LAO) scores during the 7th day of 12 mg/kg L-DOPA priming (top) and the subsequent third exposure to 7 mg/kg of L-DOPA in the same animals (middle). (G) Table of average LAO scores for all three L-DOPA priming conditions. LAO scores for the 7d and post-7d priming were taken during neurophysiological recordings, whereas the scores for the 21d priming were taken during the 21d treatment without recordings.

were implanted prior to L-DOPA exposure. Neural recordings began one week following implantation.

Neurophysiological recordings:

A multi-channel data acquisition system (KJE-1001, Amplipex Ltd.) was used for neural recordings. A light-emitting diode (LED) was attached to the rat's implant for video tracking data (Manta G-033C, Allied Vision, Exton, PA). Recordings and drug injections were conducted in a polycarbonate cage (47cm x 51cm x 20cm) once per week for each animal commencing at 5 AM. Food and water were available *ad libitum*. Recordings for the 7-d priming experiments were conducted in a large (150cm x 150cm x 23cm) open field to limit artifacts from dyskinetic animals hitting cage walls.

Histology and immunohistochemistry:

Direct current stimulation (20 mA for 20 s) was used for electrolytic lesions at each recording site. Three-days following the lesion, rats were injected with a fatal dose of Euthasol (0.35 mg/kg, *i.p.*; Virbac, Fort Worth, TX) and transcardially perfused via phosphate buffered saline and 4% paraformaldehyde. A frozen microtome was used to produce coronal sections (40 µM) for tyrosine hydroxylase (TH; Bartlett *et al.*, 2016) (**Fig. 1D**) and Nissl staining (Ye *et al.*, 2018) (**Fig. 1C**) verification of dopamine-depleted striatum and electrode placement, respectively.

Data pre-processing and statistical analysis:

Raw LFP signals were acquired at 20 kHz and down sampled to 500 Hz for analysis. Absolute values of the LFP trace that exceeded 1.5 mV or the 99.98th percentile after cross-band power (2-160 Hz) summation were considered artifact and omitted from the analyses. To reduce the impact of volume-conduction, signals were locally re-referenced using a second within-region electrode (0.7 mm inter-electrode distance) at the same depth (Ye *et al.*, 2018). ANOVAs and Student's *t*-tests (α=0.05) were used to assess statistical significance. All *post-hoc* comparisons were Tukey-Kramer or Holm corrected to adjust *p*-values. All analyses were performed using MATLAB.

Analysis of spectral activity and cross-frequency coupling:

The spectral power across frequency bands was determined using a fast Fourier transform spectrogram (frequency bin=0.5 Hz, 10s Hanning window, spectrogram() in Matlab). The frequency bands used for statistical analysis were defined as follows: delta (1–4 Hz), theta (5–10 Hz), beta (15–30 Hz), low-gamma (35–55 Hz), high-gamma (70-85 Hz), broadband gamma (40-85 Hz), and HFO (120–160 Hz).

To address the issue of power-law 1/f scaling, data was normalized using the Z-transform (Cohen, 2014). The baseline mean (-32 to -2 min preceding the first injection) was subtracted from the spectral power and then divided by the standard deviation (SD) to yield a z-score.

Phase-amplitude cross-frequency coupling (PAC) was measured as described in Cohen (2014) and Ye *et al.*, (2018). First, LFP signals were filtered in the target low- and high-frequency bands using a Butterworth filter (fs=500 Hz, order=6). Phase was extracted using a Hilbert transform. Power was extracted as the envelope of the absolute value of the filtered signal. CFC

was computed as $PAC = \left| n^{-1} \sum_{t=0}^{n} a_t^{e^{i\varphi_t}} \right|$ where a is high-frequency power and ϕ is the phase of the low-frequency signal. This value was compared to values computed using a randomized shuffle control (*n*=200 permutations). The mean and SD of this null hypothesis distribution were used to convert the measured PAC score into a z score (PACz).

Data Availability

The data are available from the corresponding author upon reasonable request.

Results

Dyskinesias and oscillatory activity in PD and LID model animals

Beta oscillations (15-30 Hz) in M1 are a signature of PD. We examined baseline oscillatory activity in M1 of PD, LID (off-state), and naïve control animals (**Fig. 1E**). As expected, significant differences in beta power were observed (ANOVA, $F(2,18)=7.71$, $p=0.004$, $\eta^2=0.25$). *Post-hoc* comparisons revealed that the PD ($p=0.002$, $n=7$) and LID groups ($p=0.04$, $n=7$) had greater beta power than naïve controls ($n=8$) (**Supplementary Fig. 1**). Beta power did not differ between PD and LID animals ($p=0.11$). Amphetamine-induced rotations were observed in these animals (>5 rotations/min; **Fig. 1F**), supporting the behavioral PD phenotype. Immunohistochemical analysis verified dopamine-depletion in the PD and LID groups (**Fig. 1D**).

The 6-OHDA-lesioned animals that met rotation criteria were assigned to either PD, LID 7 d priming, or LID 21 d priming groups. Average limb, axial, and orolingual (LAO) scores during the L-DOPA on-state clearly indicated the LID phenotype in the 7 d (12 mg/kg) (75.4±5.96; Mean±S.D.), post 7 d (7 mg/kg) (71.1±7.85), and 21 d (7 mg/kg) (33.6±6.6) groups (**Fig. 2G**). LAO scores were consistent with previous literature (Bartlett et al., 2016; Dupre et al., 2016; Halje et al., 2012).

Narrow-band 80-Hz high-gamma depends on L-DOPA dose

LID is associated with a narrow-band 80-Hz activity in M1 and DLS which is correlated with AIMs onset and duration (Halje *et al.*, 2012; Dupre *et al.*, 2016). Similarly, we observed narrow-band 80-Hz oscillations in M1, DMS, and NAc on the 7th day of high-dose L-DOPA priming (**Fig. 2B**), but not on day 10 when low-dose L-DOPA was administered (**Fig. 2C**). Both high- and low-doses expressed clear LID (**Fig. 2F**). Statistical comparisons were performed by

taking mean high-gamma power (dB) in the 22-60 min post-L-DOPA window given that L-DOPA requires ~20 minutes to become active in the CNS. ANOVA and post-hoc analyses identified a strong increase in broadband high-gamma activity in M1 (**Fig. 3A**; ANOVA, $F(4,28)=12.38$, $p=0.0001$, $\eta^2=0.42$), and smaller main effects in DMS ($F(4,28)=6.56$, $p=0.03$, $\eta^2=0.16$) and NAc ($F(4,28)=8.53$, $p=0.002$, $\eta^2=0.39$). The increase in narrow-band 80-Hz power was only identified for the 12 mg/kg L-DOPA group. This is the first report to our knowledge of LID-associated 80-Hz power in the DMS. These data also indicate that lower doses of L-DOPA can induce strong LID behaviors in the absence of narrow-band 80-Hz oscillations.

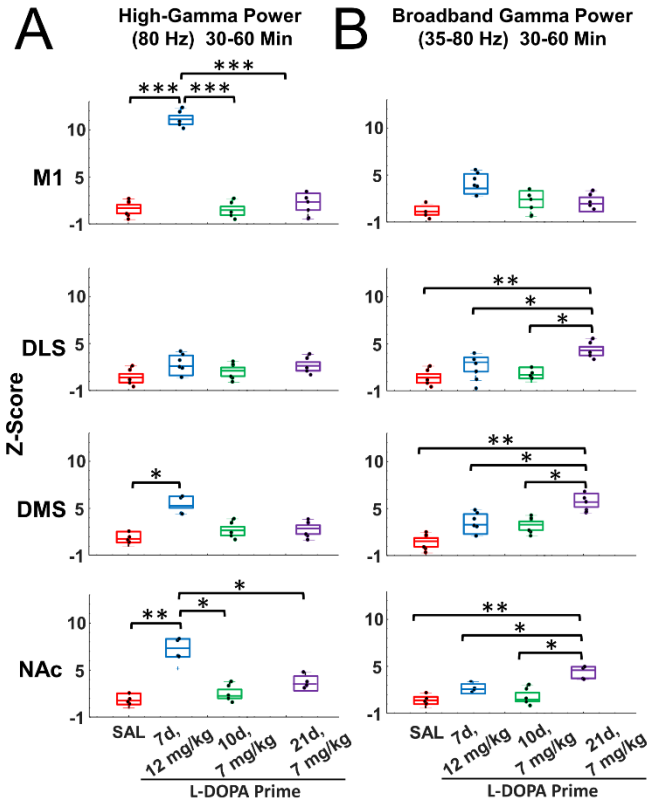

Figure 3. Priming- and dose-dependent gamma activity after L-DOPA administration in 6-OHDA-lesioned animals. (A) Data from Figure 2 B/C/E. High-gamma (80 Hz) activity in the motor cortex (M1), dorsolateral- (DLS) and dorsomedial-striatum (DMS), and nucleus accumbens (NAc) during the 22-60 min post-L-DOPA injection period for saline (red), 7d 12 mg/kg (blue), post-7d 7 mg/kg (green), and 21d 7 mg/kg (purple) priming conditions. L-DOPA (12 mg/kg, n=6) triggered significant increases in 80 Hz high-gamma compared to all conditions in the M1 and NAc (ANOVA; all p<0.05, Tukey-corrected). High-gamma was only significantly greater than SAL condition in the DMS (ANOVA; p=0.03, Tukey-corrected). (B) As in (A) but for broad-band gamma (35 – 80 Hz). broad-band gamma was significantly greater only after the 21d L-DOPA (7 mg/kg, n=7) priming protocol in the DLS and DMS compared to 7d priming and SAL (ANOVA; all p<0.05, Tukey-corrected). These data suggest differential oscillatory signatures of L-DOPA in LID animals that are dose- and priming duration-dependent.

Broadband gamma emerges after weeks-long exposure to low-dose L-DOPA

While injections of high-dose (12 mg/kg) L-DOPA induced robust narrow-band 80-Hz gamma on Day 7 of priming, inspection of mean power spectra suggested that low-dose (7 mg/kg) L-DOPA delivered on Day 10 of priming did not produce a distinct peak in the spectrogram at any frequency (**Fig. 2C**). However, after 30+ days of L-DOPA exposure in a separate group of animals, the same low-dose 7 mg/kg injection of L-DOPA appeared to increase broadband gamma power (>30 Hz) in the striatum, but not M1. To investigate this effect, we defined broadband gamma as gamma power between 35-80 Hz and assessed mean broadband activity after at least 21 days of priming (see **Supplementary Fig. 2** for a comparative analysis of low and high gamma power.). Analysis of broadband gamma in the 21+ day condition during the L-DOPA on-state revealed that broad band power increased in the NAc, DMS, and DLS, but not in M1 (**Fig. 3B,** $F_{DLS}(4,28)=8.53$, $p=0.002$, $\eta^2=0.23$; $F_{DMS}(4,28)=10.22$, $p=0.001$, $\eta^2=0.35$; $F_{NAc}(4,28)=6.31$, $p=0.02$, $\eta^2=0.15$; $F_{M1}(4,28)=2.46$, $p=0.78$, $\eta^2=0.01$). *Post-hoc* analyses within each striatal region indicated that this effect was only present after at least 21 days of priming (Tukey corrected *post-hoc* comparisons between SAL and 21-d, 7 mg/kg were significant at $p<0.01$ for DLS, DMS, and NAc), suggesting that long-duration L-DOPA exposure enhanced broadband gamma activity. These data indicate that unique spectral signatures of LID may emerge as a function of the dose used during LID induction and the duration of the priming.

Exposure to ketamine in LID animals reduces striatal gamma activity but increases M1 gamma during the L-DOPA on-state

The acute effect of ketamine injection on ongoing spectral activity in LID animals was investigated since ketamine exposure reduces AIMs scores in LID animals (Bartlett et al., 2016). LID was induced in rats using the low-dose+long-duration LID induction procedure (7 mg/kg, 21 d to establish stable and moderate LID and a cumulative LAO score of 33.6±6.6, Mean±S.D., **Fig. 2G**). These animals received a 10-hour exposure to ketamine (**Fig. 1A**) as this was the exposure protocol determined to reduce LID (Bartlett et al., 2016). Spectral activity surrounding each of the 5 ketamine injections was visualized using baseline-normalized spectrograms (**Fig. 4A**). Baseline was defined as the mean spectral power measured during the -30 to -2 min interval preceding Injection 1. The mean and SD of this activity was used to generate a z-score measure of power.

The time-course of activity in each of the targeted frequency bands surrounding Injection 1 (ketamine alone) and 5 (L-DOPA+ketamine) is presented in **Fig. 4B**.

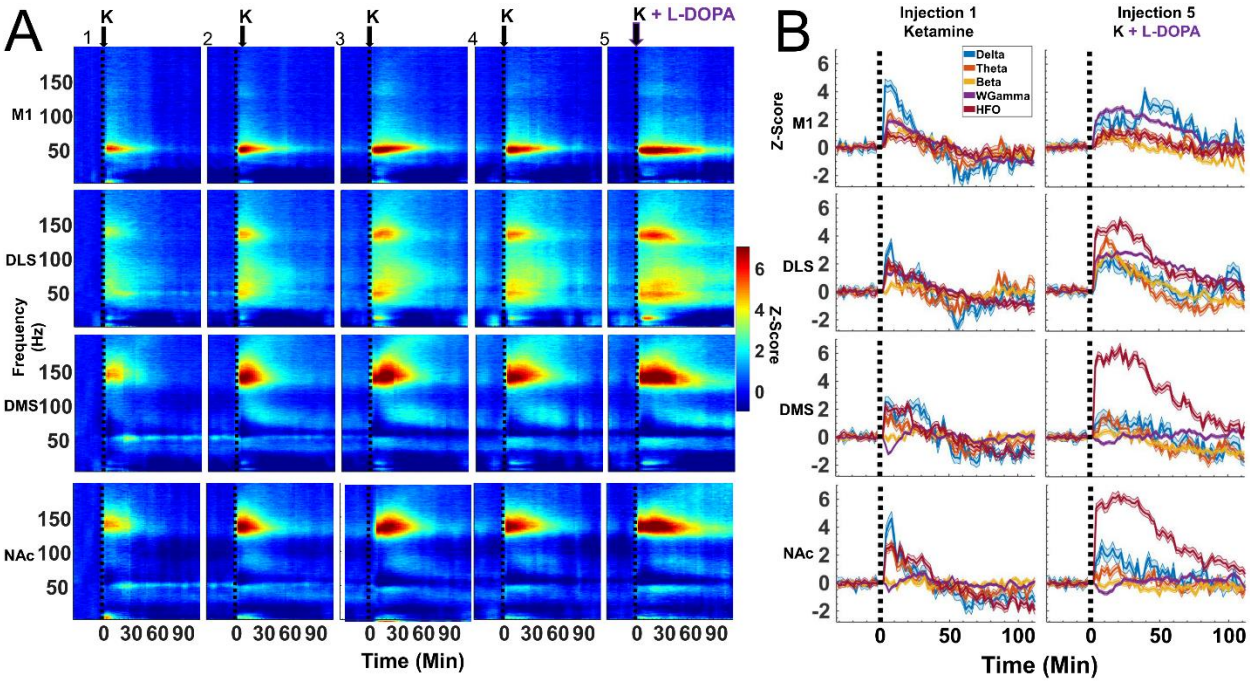

Figure 4. Average spectral responses for each successive ketamine injection in LID animals for each region. (A) Spectral responses were normalized to the pre-injection 1 baseline (-32 to -2 mins) period. In these ketamine sessions for LID animals (n=7), single injections of ketamine (20 mg/kg) were administered every two hours. The 5th/final injection was co-administration of ketamine + L-DOPA (7 mg/kg) to trigger the L-DOPA on-state. (B) Time course of spectral responses following ketamine injections 1 and 5 (ketamine + L-DOPA) by frequency band. Lines indicate mean ± SEM.

We tested the hypothesis that L-DOPA+ketamine reduces striatal broadband gamma activity that was associated with LID under the low-dose+long-duration procedure (**Fig. 2,3**). This hypothesis was explored by comparing spectral activity in LID animals on days when those animals were given L-DOPA alone (to induce LID) or L-DOPA+ketamine (**Fig. 5**). In the L-DOPA alone conditions, animals received 4 successive saline injections (2-h interval between injections), and then received a 5th injection of saline paired with L-DOPA. Neural activity was assessed during the L-DOPA on-state. In the L-DOPA+ketamine condition, animals received 4 successive injections of ketamine alone (2-h interval between injections) and were given L-DOPA+ketamine on the 5th and final injection. We predicted that broadband gamma would be reduced in the L-DOPA+ketamine condition in M1 and the striatum. The results, however, were

mixed as paired *t*-tests indicated that L-DOPA+ketamine resulted in an increase in M1 broadband-gamma ($t(6)=2.24$, $p=0.03$, $d=0.41$), a reduction of DMS ($t(6)=3.54$, $p=0.03$, $d=0.56$) and NAc ($t(6)=3.65$, $p=0.01$, $d=0.59$) gamma activity, and no difference in the DLS ($t(6)=0.98$, $p=0.13$, $d=0.11$). Consequently, the effects of ketamine on gamma in LID animals appears to be region specific and bi-directional, with gamma suppression only occurring in the medial and ventral striatum. An analysis of mean spectral power following each of the 5 injections can be found in **Supplementary Fig. 4**.

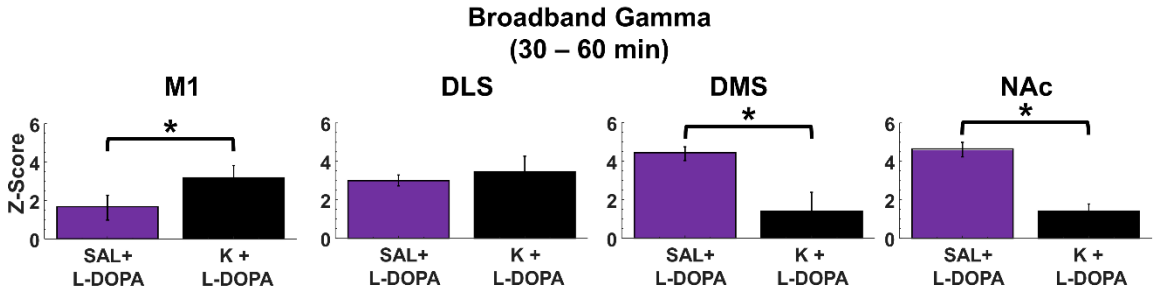

Figure 5. L-DOPA-induced broad-band gamma is reduced by ketamine in the dorsomedial striatum and nucleus accumbens. Injection of L-DOPA (7 m/kg) after 21d priming with the same dose triggered broad-band gamma oscillations (35-80 Hz, data from Figure 2E, purple bars). In the same animals (N=7), five subsequent injections of ketamine were administered with the 5th injection paired with L-DOPA (7 mg/kg, data from Figure 4A/B, black bars). Paired t-test showed ketamine did not reduce L-DOPA-induced broad-band gamma in the motor cortex or dorsolateral striatum. However, broad-band gamma was significantly reduced in the dorsomedial striatum (p=0.01) and nucleus accumbens (p=0.01).

After investigating the hypothesis that ketamine reduces broadband gamma, we performed exploratory analyses to identify potential relationships between ketamine+L-DOPA on other frequency bands. For example, and as suggested in **Fig. 4**, a notably large increase in ~140-Hz HFOs in DLS, DMS, and NAc was observed when ketamine was combined with L-DOPA during Injection 5 (ANOVA, all $p<0.05$, see **Supplementary Fig. 3** and **Supplemental Table 1**). It is well known that ketamine without L-DOPA induces robust HFOs (Nicolás *et al.*, 2011; Caixeta *et al.*, 2013, Ye *et al.*, 2018). Consequently, L-DOPA may enhance coordination between neurons in circuits involved in generating ketamine induced HFOs.

Previous exposure to ketamine is associated with increased M1 broadband activity during LID

In the preceding analysis the acute effects of co-administering ketamine with L-DOPA were investigated. However, a single 10-hour exposure to ketamine can reduce LID in rodent models for weeks (Bartlett et al., 2016), suggesting that ketamine induces lasting neuroplastic

changes. Consequently, we investigated whether prior exposure to ketamine, and not its acute effects, altered spectral activity during the L-DOPA on-state. Spectral activity was analyzed during the 30-60-minute interval following the SAL+L-DOPA injection. Within-subject comparisons (*n*=7) were made between sessions in which rats had either no prior exposure to ketamine and received only saline+L-DOPA ("0 K" in **Fig. 6**) to sessions when animals had previously received at least one exposure to ketamine (">1 K" in **Fig. 6**). Since the acute effects of ketamine were investigated in **Fig. 5**, sessions in which ketamine was also administered with L-DOPA were not included in this analysis.

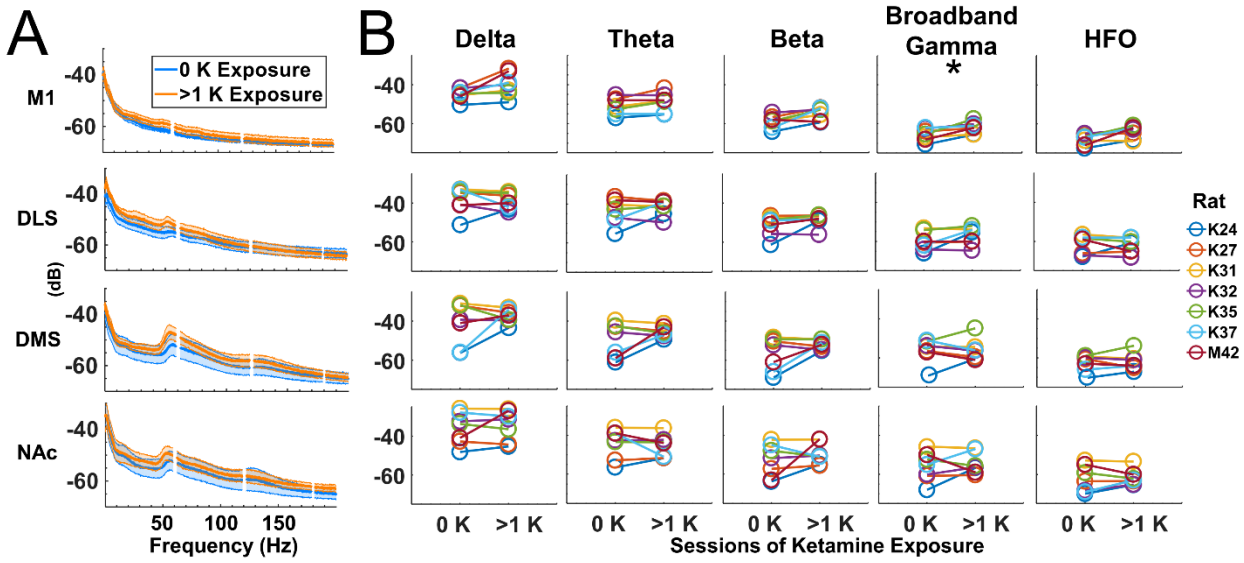

Figure 6. Repeated ketamine exposure associated with increased M1 broadband activity during LID. Repeated ketamine exposure is associated with increased M1 broadband activity during LID. (A) The 5th injection (L-DOPA, 30-60 min) of SAL sessions were used for comparison. Average power spectra (dB) for each region is shown. (B) Within-subjects comparisons (t-tests, Holm-corrected) revealed significant long-term increases in broadband gamma in M1 (p=0.03). No other significant differences were observed for any frequency band in any region.

Average spectral power (dB) for each region following L-DOPA administration is presented in **Fig. 6A**. Power-spectral responses following L-DOPA injections prior to ketamine exposure (blue) were compared to spectral responses that occurred during the weeks that followed ketamine exposures (orange). Contrary to the hypothesis that sustained ketamine exposure would reduce broadband gamma power, Holm-corrected paired *t*-tests identified an increase in spectral power in broadband gamma (p=0.03, d=1.59) in M1. No significant effects were observed in the striatum. Given that it was not feasible to have an additional group of animals that was only injected with saline for the 4 weeks of neural recording for comparison, it is conceivable that this

effect relates to some factor associated with the passage of time and not to ketamine. Even so, the fact that broadband gamma was not suppressed in this longitudinal experiment indicates that the therapeutic effects of ketamine are not a result of lasting gamma suppression during the L-DOPA on-state.

Ketamine suppresses L-DOPA-induced theta-to-high-gamma corticostriatal CFC

Theta-to-high-gamma PAC was investigated since reduced theta-to-high-gamma PAC is a feature of LID in animal models (Belić et al., 2016). Given ketamine's capacity to reduce LID, we hypothesized that ketamine administration would reduce PAC in LID rats. Theta-to-high-gamma PAC in the LID on-state (LID L-DOPA, 7 mg/kg) was compared to the condition when LID animals received ketamine (20 mg/kg) + L-DOPA (7 mg/kg, LID+K+L-DOPA). The time-course of theta-to-high-gamma PAC is presented in **Fig. 7B** (right), and group-level comparisons are presented in **Fig. 8** (right column). Inspection of the time-course of theta-to-high-gamma PAC in the LID+L-DOPA group indicated that PAC increased in M1 and the striatum relative to the pre-injection baseline (**Fig. 7B,** red lines; **Fig. 8,** red bars), and was not apparent in the LID+K+L-DOPA group (**Fig. 7**, green lines; **Fig. 8**, green bars). Statistical analysis of PAC in **Fig. 8** (right column) was performed for the 30-60 min post-injection period as this is when L-DOPA reaches peak effect. ANOVA for the 5 conditions was performed for each brain region. Main effects of condition were identified in M1, DMS, and NAc ($F_{M1}(4,28)=6.3$, $p=0.001$, $\eta^2=0.51$; $F_{DMS}(4,31)=7.12$, $p=0.0004$, $\eta^2=0.51$; $F_{NAc}(4,28)=14.8$, $p=0.0001$, $\eta^2=0.68$), but not DLS ($p>0.05$).

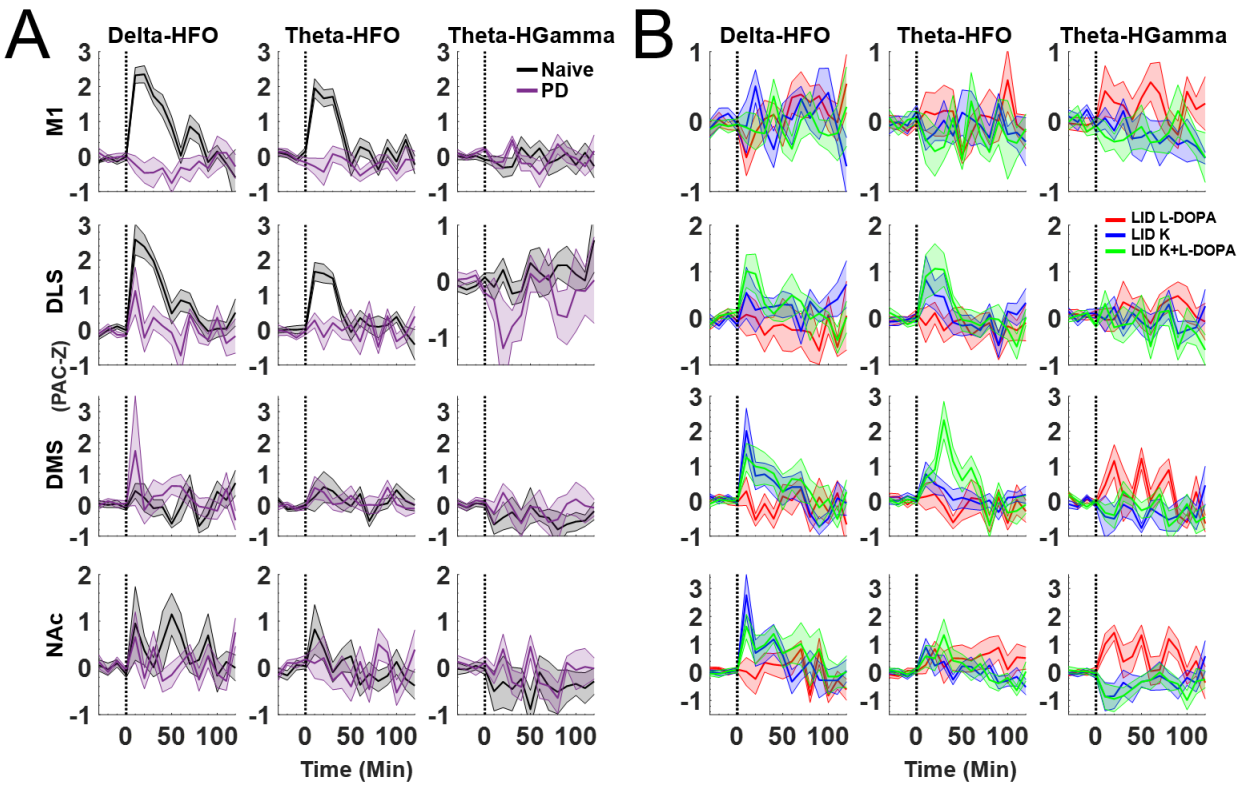

Figure 7. Ketamine induced cross-frequency coupling in naïve, 6-OHDA-lesioned, and LID animals. (A) Time course of drug-induced CFC in the motor cortex, dorso-lateral/medial striatum, and nucleus accumbens. Data shown are averages of the 4th injection of ketamine in naïve (black) and 6-OHDA-lesioned (purple) animals. (B) As in (A) but for LID animals receiving injections of L-DOPA alone (red), ketamine alone (blue), or ketamine + L-DOPA (green).

Theta-to-high-gamma PAC in LID animals following L-DOPA administration (red bars) was significantly reduced after co-administration with ketamine (green bars) in M1, DMS, and NAc (Tukey *post-hoc* corrected: p_{M1}=0.02, d=1.56, p_{DMS}=0.01, d=2.39, p_{NAc}=0.0005, d=4.54), but not DLS (p>0.05). This effect was also observed when ketamine was delivered without L-DOPA in M1, DMS, and NAc (blue bars, LID off state; p_{M1}=0.02, d=1.56, p_{DMS}=0.01, d=2.39, p_{NAc}=0.0005, d=4.54), but not DLS (p>0.05). These data suggest that ketamine impacts the oscillatory signature of LID by altering cross-frequency interactions and, specifically, by reducing theta-to-high-gamma PAC.

Ketamine induces delta-HFO and theta-HFO cross-frequency coupling in naïve but not in PD and LID animals

Cross-frequency coupling is believed to support neural communication and neural plasticity by organizing the timing of action potentials (Canolty and Knight, 2010; Lisman and

Jensen, 2013). Excessive CFC can also indicate circuit dysfunction. For example, increased theta- and delta-to-high-gamma phase-amplitude coupling is a signature of PD in primate models (Devergnas et al., 2019). Because acute exposure to ketamine is known to produce strong delta-HFO and theta-HFO coupling in the cortex and striatum (Cordon et al., 2015), we investigated whether acute exposure to ketamine alters CFC in naïve, PD, and LID hemi-lesioned rats.

In agreement with previous reports (Ye et al., 2018), ketamine injections produced robust delta- and theta-to-HFO PAC in M1 and striatum of naïve rats (**Fig. 7,** and black bars in **Supplementary Fig. 5**). Surprisingly, ketamine-induced delta- and theta-HFO CFC was absent in PD and LID rats (**Fig. 8, Supplementary Fig. 5:** black bars compared to PD and LID conditions). ANOVA identified a main effect of experimental condition (*e.g.*, naïve, PD, LID) and CFC frequency band in M1 and DLS (M1: delta-HFO: $F(4,28)=12.2$, $p=0.0001$, $\eta^2=0.95$; theta-HFO: $F(4,28)=32.0$, $p=0.0002$, $\eta^2=0.84$; DLS: delta-HFO: $F(4,31)=29.6$, $p=0.0001$, $\eta^2=0.81$; theta-HFO PAC: $F(4,31)=13.82$, $p=0.0002$, $\eta^2=0.67$; NAc: delta-HFO: $F(4,31)=15.36$, $p=0.001$, $\eta^2=0.75$). *Post-hoc* comparisons indicated that increased delta-HFO PAC in naïve (M1, DLS, and NAc, all $p<0.001$) but not PD/LID animals. The absence of coupling with HFOs in LID was surprising as HFOs and increased theta and delta-band power was observed following each ketamine injection in the LID animals (**Fig. 4**). These results suggest that the low and high frequency oscillators activated by ketamine exposure become decoupled after prolonged dopamine depletion.

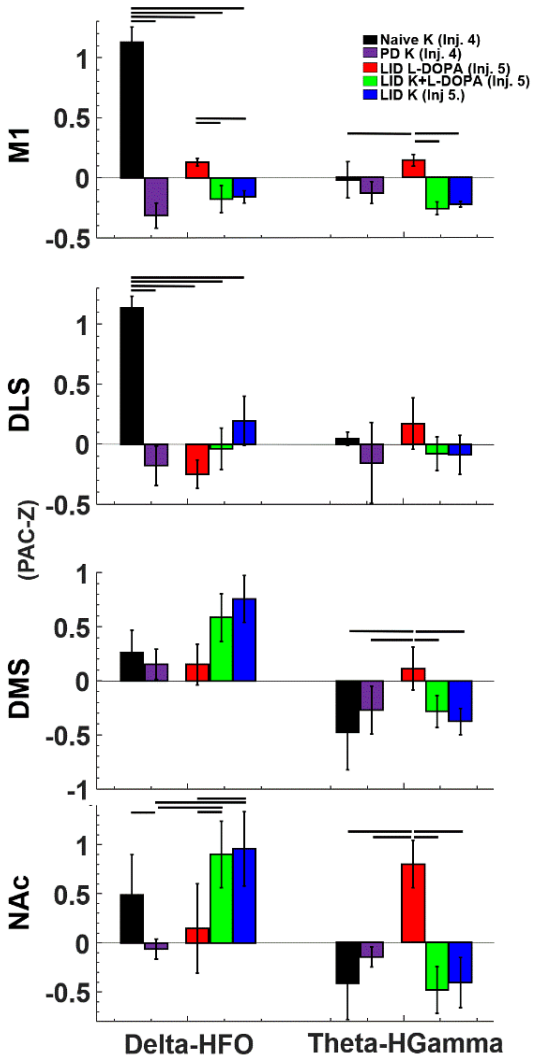

Figure 8. Ketamine suppresses cross-frequency coupling associated with LID. Data from (A) and (B) averaged between 30 – 60 min post-drug injection. ANOVA was used for all statistics with Tukey-Kramer post-hoc correction. In the motor cortex, the 4th injection of ketamine in naïve animals triggered significant increases in delta-HFO CFC compared to all conditions (all $p<0.05$). In LID animals, co-injection of L-DOPA + ketamine (green) significantly reduced delta-HFO coupling compared to L-DOPA alone (red) ($p=0.04$). Theta-high gamma CFC was significantly reduced in the motor cortex, DMS, and NAc following an injection of ketamine in naïve animals (black) and in LID animals (blue) even with L-DOPA on board (green) (all $p<0.05$). This suggests that ketamine selectively reduces CFC in the on-state of LID animals.

Discussion

L-DOPA-induced dyskinesias are a debilitating consequence of dopamine-replacement therapy for PD. Although there is an abundance of research into the cellular and synaptic origins of LID, far less is known about how LID impacts systems-level circuits and neural synchrony. We investigated the oscillatory signatures of LID and explored how different LID priming procedures

affect these signatures. Our first observation was that the LID priming procedure itself impacts neural synchrony. We discovered that while short-term high-dose L-DOPA priming induced focal corticostriatal 80-Hz oscillations (Dupre et al., 2016; Halje et al., 2012), a common low-dose procedure did not, and, instead, increased non-oscillatory broadband gamma activity in the striatum. We then explored how this activity was affected by ketamine, given evidence that ketamine reduces LID (Bartlett et al., 2016). We found that ketamine exposure during the LID on-state suppressed striatal broadband gamma, but enhanced broadband gamma in M1. This suggests that ketamine's potential therapeutic effects are region specific. Similarly, we found that LID on-state was associated with theta-to-high-gamma CFC in M1 which was suppressed by ketamine. An unexpected finding was that while ketamine induced robust theta- and delta-HFO CFC in naïve rats (Caixeta et al., 2013; Cordon et al., 2015; Ye et al., 2018), no such coupling was observed in PD or LID animals, despite these animals exhibiting robust HFOs. This suggests that prolonged dopamine depletion decouples neuronal networks involved in cross-band synchrony.

L-DOPA dose determines the spectral signature of LID

While low-dose L-DOPA administration (6-7 mg/kg) is a common procedure for priming and LID-induction (Cenci *et al.*, 1998; Dekundy *et al.*, 2007; Bartlett *et al.*, 2016), LID-associated oscillatory activity has only been investigated using high-doses of L-DOPA (12 mg/kg) (Dupre et al., 2016; Halje et al., 2012; Tamte et al., 2016). Using the high-dose procedure, we replicated previous reports that LID is accompanied by focal 80-Hz oscillations in M1, DMS, and DLS (Dupre et al., 2016; Halje et al., 2012; Tamte et al., 2016). Surprisingly, these 80-Hz oscillations were absent during the LID on-state under low-dose priming. Instead, these animals expressed increased theta-to-high-gamma CFC during the LID on-state and non-oscillatory broadband gamma activity that developed gradually over 30+ days of priming. Thus, L-DOPA can induce fundamentally distinct spectral states in animals expressing LID that depend on the dose and duration of exposure.

Focal 80-Hz gamma following high-dose L-DOPA priming

Focal 80-Hz oscillations suggest tight temporal coordination between local networks of coupled inhibitory neurons (I-I) (Brunel and Wang, 2003; Buzsáki and Wang, 2012). In animal models, 80-Hz oscillations and L-DOPA-induced dyskinesias are reduced following the application D1R antagonists to the cortical surface (Halje et al., 2012). This suggests that activation

of cortical D1 receptors can trigger and/or sustain these oscillations. D1 receptors (Towers and Hestrin, 2008) and NMDA receptors (Lim et al., 2014) are expressed on M1 GABAergic interneurons and striatal medium spiny neurons (MSNs) which may partly explain why D1R and NMDAR antagonists interfere with these oscillations (Kirli et al., 2014) and why NMDAR antagonists reduce LID in human patients (Goetz et al., 2005; Oertel et al., 2017). As with Tamte *et al*. (2016), we observed 80-Hz gamma outside of M1 and specifically in the DMS. This suggests that 80-Hz gamma is either transmitted to DMS from M1 (Richter et al., 2013) or generated locally within the DMS. The latter possibility is conceivable as >95% of striatal neurons are inhibitory and tightly coupled and so, like M1, may be capable of sustaining high-frequency gamma oscillations. Finally, it is conceivable that focal gamma is mediated by dopamine D4 receptors in the basal ganglia (Bello et al., 2019) as D4R-mediated gamma oscillations have been observed in the hippocampus (Andersson et al., 2012).

Broadband gamma in LID emerges after weeks of low-dose priming

While clear 80-Hz oscillations emerged after 10 days of high-dose L-DOPA administration, no such activity was identified after 10 days of low-dose administration. Instead, low-dose L-DOPA exposure produced broadband desynchronized activity after 30 days of regular low-dose priming. Unlike 80-Hz gamma, broadband gamma was present in the striatum but not in M1 (**Fig. 2,3**). To our knowledge, this is the first report of a new LID spectral signature using the low-dose 21-d priming procedure. The gradual development of broadband gamma with repeated L-DOPA exposure suggests neuroplastic changes resulting from cycling dopamine levels (Calabresi et al., 2015) that may drive the reorganization of striatal circuits through the activities of fast-spiking interneurons (Berke, 2011). Similar high-frequency broadband activity has been interpreted as increased action-potential firing or an altered balance between excitation and inhibition (Rubenstein and Merzenich, 2003; Voytek et al., 2015). These ideas are consistent with the observation that L-DOPA treatment increases direct pathway activity (Albin et al., 1989; DeLong, 1990), and because optogenetic and chemogenetic manipulations that increase striatal direct-pathway activity produce LID in animal models (Alcacer et al., 2017; Perez et al., 2017; Rothwell et al., 2015). How this excitability emerges is an open question. It is conceivable that persistent L-DOPA treatment and chronically elevated dopamine levels increase dopamine-mediated plasticity in the absence of sensorimotor input (Fieblinger et al., 2014; Picconi et al.,

2003; Shen et al., 2008). Plasticity in the absence of input could disrupt the mapping of striatal responses to afferent input and result in less organized broadband striatal activity.

LID-associated broadband gamma was reduced when L-DOPA was co-administration with ketamine

Given evidence that ketamine can reduce dyskinesias, we predicted that spectral signatures of LID would decrease after ketamine administration. Specifically, we hypothesized that ketamine administration would reduce the striatal broadband gamma activity we observed during LID in animals exposed to the 21-day low-dose priming procedure. In agreement, broadband gamma was reduced in DMS and NAc in the L-DOPA+ketamine condition relative to the L-DOPA alone condition (**Fig. 5**). Such suppression was not observed in DLS and M1. Broadband gamma is linked to several physiological processes (Buzsáki and Wang, 2012) including enhanced neural excitability (Fries et al., 2007). L-DOPA treatment is believed to increase direct pathway activity (Albin et al., 1989; DeLong, 1990), and increased direct-pathway neural activity may be a component of the observed increase in broadband power in LID animal models (Alcacer et al., 2017; Perez et al., 2017; Rothwell et al., 2015). Consequently, it is conceivable that ketamine reduces pathological activation of the direct pathway to exert anti-dyskinetic effects. It is less clear why this effect is most prominent in NAc and DMS, but not DLS.

The ketamine-alone and ketamine+L-DOPA conditions all resulted in increased M1 broadband gamma (**Fig. 5**). Similar responses to ketamine and other NMDAR antagonists have been reported (Nicolás *et al.*, 2011; Hunt and Kasicki, 2013, Ye *et al.*, 2018) (**Fig. 4**). Gamma-generation in the cortex by ketamine could result from its antagonism of NMDARs on parvalbumin-expressing (PV) GABAergic interneurons as these NMDARs have a high affinity for ketamine (Hunt and Kasicki, 2013). Antagonism of NMDARs has been proposed to reduce PV-neuron activity and consequently, disinhibit M1 principal cells (Buzsáki and Wang, 2012; Homayoun and Moghaddam, 2007; Korotkova et al., 2010; Pinault, 2008). This could engage local networks of non-parvalbumin inhibitory cells, contributing to gamma generation (Whittington et al., 1995). Moreover, patient and preclinical models of LID have shown increased glutamatergic activity (Oh *et al.*, 1998; Chase and Oh, 2000; Calon *et al.*, 2002). The combined effect of ketamine+L-DOPA on glutamatergic neurons may partially account for enhanced oscillatory

activity. Dopamine may also be involved as ketamine-induced locomotion and gamma in M1 were eliminated when ketamine was delivered after administration of a D1R antagonist (Ye *et al.*, 2018).

Ketamine exposure produces a days-long increase in LID on-state broadband activity in the motor cortex

Ketamine exposure can induce neuroplastic changes that endure for weeks following a single exposure in rats (Li et al., 2010). Furthermore, a single 10-hour ketamine exposure can produce a weeks-long reduction in an animal model of LID (Bartlett et al., 2016), suggesting that ketamine-induced neuroplastic changes contribute to reduced LID. To investigate this, we examined LID on-state spectral activity for the days surrounding the first exposure to ketamine. We found that broadband activity in activity increased in the days that followed the first 10-hour exposure to ketamine (**Fig. 6**). A limitation of our study is that L-DOPA-induced AIMs were not scored during the recording period. Consequently, we cannot directly correlate within-session broadband activity with LID severity. While it is unclear why prior exposure to ketamine selectively increased broadband gamma activity in M1 but not the striatum, it is conceivable that increased synaptogenesis and brain-derived neurotrophic factor (BDNF) production (Phoumthipphavong et al., 2016; Yang et al., 2013) in the cortex are responsible.

L-DOPA-induced theta to high-gamma CFC in PD and LID rats is suppressed by ketamine

In healthy animals, CFC may facilitate information transfer between brain regions (Canolty and Knight, 2010), or organize the timing of neural ensemble activity to support learning and memory (Lisman and Jensen, 2013). The potential roles of CFC in LID are largely unexplored, and only one study has investigated CFC in LID using the high-dose condition (Belić et al., 2016). This study identified reduced theta-to-80-Hz coupling in LID animals despite these animals expressing strong 80-Hz oscillations. Like Belić *et al*., we hypothesized that theta-to-high-gamma activity would be suppressed in LID rats, and that the novel broadband gamma activity we observed in LID under 7 mg/kg priming would be decoupled from low-frequency oscillations. Instead, we observed that theta-to-high-gamma CFC increased in M1, DLS, and NAc of LID animals (**Fig. 8**), suggesting that the priming procedure and dose can trigger distinct oscillatory neural states that are not a simple linear function of L-DOPA dosage. Regarding broadband

gamma, we did not observe theta-to-broadband gamma CFC in LID animals primed for 21+ days with 7 mg/kg L-DOPA, suggesting that theta-to-broadband gamma CFC is not a signature of LID.

Ketamine enhances delta-HFO and theta-HFO cross-frequency coupling in naïve but not PD and LID animals

Multiple groups have reported that sub-anesthetic exposure to ketamine and other NMDAR antagonists induces strong HFOs (120–160 Hz) in the striatum (Olszewski *et al.*, 2013; Cordon *et al.*, 2015; Hunt *et al.*, 2015, Ye *et al.*, 2018), cortex (Cordon et al., 2015; Nicolás et al., 2011), and hippocampus (Caixeta et al., 2013). Some have also reported that these HFOs are coupled to the phase of delta and theta oscillations (Caixeta *et al.*, 2013; Cordon *et al.*, 2015, Ye *et al.*, 2018). In support of this, we observed robust ketamine induced HFOs in naïve, PD, and LID rats in M1 and the striatum (**Fig. 4**). Surprisingly, while delta- and theta-HFO CFC was clear in naïve rats, such coupling was not present in the PD or LID animals (**Fig. 8**). This suggests that prolonged dopamine depletion reconfigures circuits involved in synchronizing low-frequency oscillations with HFOs. It is conceivable that decoupling between delta/theta oscillations and HFOs is a physiological indicator of PD progression similar to beta-band synchrony (Brown, 2007). Future studies are required to determine if ketamine-induced delta- and theta-HFO CFC changes with disease progression.

Conclusions

Our findings provide new insights and a more nuanced view of how PD and LID impacts neural coordination in corticostriatal circuits. While we replicated the observation that focal 80-Hz oscillations are a robust signature of LID, we also found that this signature depends on the dose of L-DOPA administered. In fact, no 80-Hz activity was observed during the LID on-state in animals primed with the low-dose procedure. Instead, L-DOPA-induced broadband gamma activity emerged after weeks of low-dose priming. These differences suggest that the neural signatures of L-DOPA induced dyskinesia do not lie on a continuum that depends on dose, but that the dose can produce distinct threshold-dependent neuronal states in corticostriatal circuits. This is supported by our observation that high-dose priming results in suppressed theta-to-high-gamma CFC while low-dose priming enhanced CFC. Enhanced CFC in the low-dose condition was also suppressed by ketamine, suggesting that a component of ketamine's anti-dyskinetic effect could

be through suppression of theta-to-high-gamma CFC. Therefore, the results have clinical relevance for individuals with PD, complementing currently ongoing clinical testing of sub-anesthetic ketamine for the treatment of LID by our group.

Acknowledgements

We would like to give special thanks to Matthew Schmit, Paulluvi Bahl, Maddy Otto, and the collective undergraduates of the Cowen and Falk-Sherman laboratories for their contributions. MJB would like to thank the Society for Neuroscience's Neuroscience Scholars Program for his Fellowship.

Funding

This work was supported by the Evelyn F. McKnight Brain Institute, Arizona Biomedical Research Commission Grant ADHS18-198846 (SJS, TF), NIH R56-NS109608 (TF, SLC), and T35-HL007479 (MJB).

Competing interests

Authors TY, MJB and SLC report no competing interests. SJS and TF have a pending patent application for the use of ketamine as a novel treatment for levodopa-induced dyskinesia associated with Parkinson's disease.

References

Albin, R.L., Young, A.B., Penney, J.B., 1989. The functional anatomy of basal ganglia disorders. Trends Neurosci. 12, 366–75.

Alcacer, C., Andreoli, L., Sebastianutto, I., Jakobsson, J., Fieblinger, T., Cenci, M.A., 2017. Chemogenetic stimulation of striatal projection neurons modulates responses to Parkinson's disease therapy. J. Clin. Invest. 127, 720–734. https://doi.org/10.1172/JCI90132

Alonso-Frech, F., Zamarbide, I., Alegre, M., Rodríguez-Oroz, M.C., Guridi, J., Manrique, M., Valencia, M., Artieda, J., Obeso, J.A., 2006. Slow oscillatory activity and levodopa-induced dyskinesias in Parkinson's disease. Brain 129, 1748–57. https://doi.org/10.1093/brain/awl103

Andersson, R.H., Johnston, A., Herman, P.A., Winzer-Serhan, U.H., Karavanova, I., Vullhorst, D., Fisahn, A., Buonanno, A., 2012. Neuregulin and dopamine modulation of hippocampal gamma oscillations is dependent on dopamine D4 receptors. Proc. Natl. Acad. Sci. 109, 13118–13123. https://doi.org/10.1073/pnas.1201011109

Andrade, C., 2017. Ketamine for Depression, 1: Clinical Summary of Issues Related to Efficacy, Adverse Effects, and Mechanism of Action. J. Clin. Psychiatry 78, e415–e419. https://doi.org/10.4088/JCP.17f11567

Bartlett, M.J., Joseph, R.M., LePoidevin, L.M., Parent, K.L., Laude, N.D., Lazarus, L.B., Heien, M.L., Estevez, M., Sherman, S.J., Falk, T., 2016. Long-term effect of sub-anesthetic ketamine in reducing L-DOPA-induced dyskinesias in a preclinical model. Neurosci. Lett. 612, 121–5. https://doi.org/10.1016/j.neulet.2015.11.047

Belić, J.J., Halje, P., Richter, U., Petersson, P., Kotaleski, J.H., 2016. Untangling cortico-striatal connectivity and cross-frequency coupling in L-DOPA-induced dyskinesia. Front. Syst. Neurosci. 10, 1–12. https://doi.org/10.3389/fnsys.2016.00026

Bello, F. Del, Giannella, M., Giorgioni, G., Piergentili, A., Quaglia, W., 2019. Receptor ligands as helping hands to l-dopa in the treatment of parkinson's disease. Biomolecules 9. https://doi.org/10.3390/biom9040142

Berke, J.D., 2011. Functional properties of striatal fast-spiking interneurons. Front. Syst. Neurosci.

5, 45. https://doi.org/10.3389/fnsys.2011.00045

Brown, P., 2007. Abnormal oscillatory synchronisation in the motor system leads to impaired movement. Curr. Opin. Neurobiol. 17, 656–64. https://doi.org/10.1016/j.conb.2007.12.001

Brunel, N., Wang, X.J., 2003. What determines the frequency of fast network oscillations with irregular neural discharges? I. Synaptic dynamics and excitation-inhibition balance. J. Neurophysiol. 90, 415–430. https://doi.org/10.1152/jn.01095.2002

Buzsáki, G., Wang, X.-J., 2012. Mechanisms of Gamma Oscillations. Annu. Rev. Neurosci. 35, 203–225. https://doi.org/10.1146/annurev-neuro-062111-150444

Caixeta, F. V, Cornélio, A.M., Scheffer-Teixeira, R., Ribeiro, S., Tort, A.B.L., 2013. Ketamine alters oscillatory coupling in the hippocampus. Sci. Rep. 3, 2348. https://doi.org/10.1038/srep02348

Calabresi, P., Ghiglieri, V., Mazzocchetti, P., Corbelli, I., Picconi, B., 2015. Levodopa-induced plasticity: a double-edged sword in Parkinson's disease? Philos. Trans. R. Soc. Lond. B. Biol. Sci. 370. https://doi.org/10.1098/rstb.2014.0184

Calon, F., Birdi, S., Rajput, A.H., Hornykiewicz, O., Bédard, P.J., Di Paolo, T., 2002. Increase of preproenkephalin mRNA levels in the putamen of Parkinson disease patients with levodopa-induced dyskinesias. J. Neuropathol. Exp. Neurol. 61, 186–196. https://doi.org/10.1093/jnen/61.2.186

Canolty, R.T., Knight, R.T., 2010. The functional role of cross-frequency coupling. Trends Cogn. Sci. 14, 506–15. https://doi.org/10.1016/j.tics.2010.09.001

Carta, M., Lindgren, H.S., Lundblad, M., Stancampiano, R., Fadda, F., Cenci, M.A., 2006. Role of striatal L-DOPA in the production of dyskinesia in 6-hydroxydopamine lesioned rats. J. Neurochem. 96, 1718–1727. https://doi.org/10.1111/j.1471-4159.2006.03696.x

Cenci, M.A., Lee, C.S., Björklund, A., 1998. L-DOPA-induced dyskinesia in the rat is associated with striatal overexpression of prodynorphin- and glutamic acid decarboxylase mRNA. Eur. J. Neurosci. 10, 2694–2706. https://doi.org/10.1046/j.1460-9568.1998.00285.x

Chase, T.N., Oh, J.D., 2000. Striatal dopamine- and glutamate-mediated dysregulation in experimental parkinsonism. Trends Neurosci. 23, 86–91. https://doi.org/10.1016/S1471-

1931(00)00018-5

Cordon, I., Nicolás, M.J., Arrieta, S., Lopetegui, E., López-Azcárate, J., Alegre, M., Artieda, J., Valencia, M., 2015. Coupling in the cortico-basal ganglia circuit is aberrant in the ketamine model of schizophrenia. Eur. Neuropsychopharmacol. 25, 1375–87. https://doi.org/10.1016/j.euroneuro.2015.04.004

Cotzias, G., Papvasiliou, P., Gellene, R., 1969. Modification of Parkinsonism -- Chronic Treatment with L-DOPA. New Engl. J. Med. 280, 337–345. https://doi.org/10.1056/NEJM198107023050102

Dekundy, A., Lundblad, M., Danysz, W., Cenci, M.A., 2007. Modulation of L-DOPA-induced abnormal involuntary movements by clinically tested compounds: further validation of the rat dyskinesia model. Behav. Brain Res. 179, 76–89. https://doi.org/10.1016/j.bbr.2007.01.013

DeLong, M.R., 1990. Primate models of movement disorders of basal ganglia origin. Trends Neurosci. https://doi.org/10.1016/0166-2236(90)90110-V

Devergnas, A., Caiola, M., Pittard, D., Wichmann, T., 2019. Cortical Phase–Amplitude Coupling in a Progressive Model of Parkinsonism in Nonhuman Primates. Cereb. Cortex 29, 167–177. https://doi.org/10.1093/cercor/bhx314

Diamond, P.R., Farmery, A.D., Atkinson, S., Haldar, J., Williams, N., Cowen, P.J., Geddes, J.R., McShane, R., 2014. Ketamine infusions for treatment resistant depression: a series of 28 patients treated weekly or twice weekly in an ECT clinic. J. Psychopharmacol. 28, 536–544. https://doi.org/10.1177/0269881114527361

Dupre, K.B., Cruz, A. V., McCoy, A.J., Delaville, C., Gerber, C.M., Eyring, K.W., Walters, J.R., 2016. Effects of L-dopa priming on cortical high beta and high gamma oscillatory activity in a rodent model of Parkinson’s disease. Neurobiol. Dis. 86, 1–15. https://doi.org/10.1016/j.nbd.2015.11.009

Fieblinger, T., Graves, S.M., Sebel, L.E., Alcacer, C., Plotkin, J.L., Gertler, T.S., Chan, C.S., Heiman, M., Greengard, P., Cenci, M.A., Surmeier, D.J., 2014. Cell type-specific plasticity of striatal projection neurons in parkinsonism and L-DOPA-induced dyskinesia. Nat. Commun. 5, 1–15. https://doi.org/10.1038/ncomms6316

Fries, P., Nikolić, D., Singer, W., 2007. The gamma cycle. Trends Neurosci. 30, 309–16. https://doi.org/10.1016/j.tins.2007.05.005

Goetz, C.G., Poewe, W., Rascol, O., Sampaio, C., 2005. Evidence-based medical review update: Pharmacological and surgical treatments of Parkinson's disease: 2001 to 2004. Mov. Disord. https://doi.org/10.1002/mds.20464

Halje, P., Tamte, M., Richter, U., Mohammed, M., Cenci, M.A., Petersson, P., 2012. Levodopa-Induced Dyskinesia Is Strongly Associated with Resonant Cortical Oscillations. J. Neurosci. 32, 16541–16551. https://doi.org/10.1523/JNEUROSCI.3047-12.2012

Homayoun, H., Moghaddam, B., 2007. NMDA Receptor Hypofunction Produces Opposite Effects on Prefrontal Cortex Interneurons and Pyramidal Neurons. J. Neurosci. 27, 11496–11500. https://doi.org/10.1523/JNEUROSCI.2213-07.2007

Hunt, M.J., Kasicki, S., 2013. A systematic review of the effects of NMDA receptor antagonists on oscillatory activity recorded in vivo. J. Psychopharmacol. 27, 972–86. https://doi.org/10.1177/0269881113495117

Hunt, M.J., Olszewski, M., Piasecka, J., Whittington, M.A., Kasicki, S., 2015. Effects of NMDA receptor antagonists and antipsychotics on high frequency oscillations recorded in the nucleus accumbens of freely moving mice. Psychopharmacology (Berl). 232, 4525–4535. https://doi.org/10.1007/s00213-015-4073-0

Kaufman, M.B., 2019. Pharmaceutical Approval Update. P T 44, 337–339.

Kirli, K.K., Ermentrout, G.B., Cho, R.Y., 2014. Computational study of NMDA conductance and cortical oscillations in schizophrenia. Front. Comput. Neurosci. 8, 1–10. https://doi.org/10.3389/fncom.2014.00133

Korotkova, T., Fuchs, E.C., Ponomarenko, A., von Engelhardt, J., Monyer, H., 2010. NMDA receptor ablation on parvalbumin-positive interneurons impairs hippocampal synchrony, spatial representations, and working memory. Neuron 68, 557–69. https://doi.org/10.1016/j.neuron.2010.09.017

Li, N., Lee, B., Liu, R.-J., Banasr, M., Dwyer, J.M., Iwata, M., Li, X.-Y., Aghajanian, G., Duman, R.S., 2010. mTOR-dependent synapse formation underlies the rapid antidepressant effects of NMDA antagonists. Science 329, 959–64. https://doi.org/10.1126/science.1190287

Lim, S.A.O., Kang, U.J., McGehee, D.S., 2014. Striatal cholinergic interneuron regulation and circuit effects. Front. Synaptic Neurosci. 6, 1–23. https://doi.org/10.3389/fnsyn.2014.00022

Lisman, J.E., Jensen, O., 2013. The Theta-Gamma Neural Code. Neuron 77, 1002–1016. https://doi.org/10.1016/j.neuron.2013.03.007

Litvak, V., Jha, A., Eusebio, A., Oostenveld, R., Foltynie, T., Limousin, P., Zrinzo, L., Hariz, M.I., Friston, K., Brown, P., 2011. Resting oscillatory cortico-subthalamic connectivity in patients with Parkinson's disease. Brain 134, 359–74. https://doi.org/10.1093/brain/awq332

Lopez-Azcarate, J., Tainta, M., Rodriguez-Oroz, M.C., Valencia, M., Gonzalez, R., Guridi, J., Iriarte, J., Obeso, J.A., Artieda, J., Alegre, M., 2010. Coupling between Beta and High-Frequency Activity in the Human Subthalamic Nucleus May Be a Pathophysiological Mechanism in Parkinson's Disease. J. Neurosci. 30, 6667–6677. https://doi.org/10.1523/JNEUROSCI.5459-09.2010

Lundblad, M., Andersson, M., Winkler, C., Kirik, D., Wierup, N., Cenci Nilsson, M.A., 2002. Pharmacological validation of behavioural measures of akinesia and dyskinesia in a rat model of Parkinson's disease. Eur. J. Neurosci. 15, 120–132. https://doi.org/10.1046/j.0953-816x.2001.01843.x

Nash, J.E., Brotchie, J.M., 2002. Characterisation of striatal NMDA receptors involved in the generation of Parkinsonian symptoms: Intrastriatal microinjection studies in the 6-OHDA-lesioned rat. Mov. Disord. 17, 455–466. https://doi.org/10.1002/mds.10107

Nicolás, M.J., López-Azcárate, J., Valencia, M., Alegre, M., Pérez-Alcázar, M., Iriarte, J., Artieda, J., 2011. Ketamine-induced oscillations in the motor circuit of the rat basal ganglia. PLoS One 6, e21814. https://doi.org/10.1371/journal.pone.0021814

Niesters, M., Martini, C., Dahan, A., 2014. Ketamine for chronic pain: risks and benefits. Br. J. Clin. Pharmacol. 77, 357–67. https://doi.org/10.1111/bcp.12094

Oertel, W., Eggert, K., Pahwa, R., Tanner, C.M., Hauser, R.A., Trenkwalder, C., Ehret, R., Azulay, J.P., Isaacson, S., Felt, L., Stempien, M.J., 2017. Randomized, placebo-controlled trial of ADS-5102 (amantadine) extended-release capsules for levodopa-induced dyskinesia in Parkinson's disease (EASE LID 3). Mov. Disord. 32, 1701–1709. https://doi.org/10.1002/mds.27131

Oh, J.D., Russell, D., Vaughan, C.L., Chase, T.N., 1998. Enhanced tyrosine phosphorylation of striatal NMDA receptor subunits: Effect of dopaminergic denervation and L-DOPA administration. Brain Res. 813, 150–159. https://doi.org/10.1016/S0006-8993(98)01049-X

Olanow, C.W., Stern, M.B., Sethi, K., 2009. The scientific and clinical basis for the treatment of Parkinson disease (2009). Neurology 72, S1-136. https://doi.org/10.1212/WNL.0b013e3181a1d44c

Olszewski, M., Dolowa, W., Matulewicz, P., Kasicki, S., Hunt, M.J., 2013. NMDA receptor antagonist-enhanced high frequency oscillations: Are they generated broadly or regionally specific? Eur. Neuropsychopharmacol. 23, 1795–1805. https://doi.org/10.1016/j.euroneuro.2013.01.012

Perez, X.A., Zhang, D., Bordia, T., Quik, M., 2017. Striatal D1 medium spiny neuron activation induces dyskinesias in parkinsonian mice. Mov. Disord. 32, 538–548. https://doi.org/10.1002/mds.26955

Phoumthipphavong, V., Barthas, F., Hassett, S., Kwan, A.C., 2016. Longitudinal Effects of Ketamine on Dendritic Architecture In Vivo in the Mouse Medial Frontal Cortex. eneuro 3, ENEURO.0133-15.2016. https://doi.org/10.1523/ENEURO.0133-15.2016

Picconi, B., Centonze, D., Håkansson, K., Bernardi, G., Greengard, P., Fisone, G., Cenci, M.A., Calabresi, P., 2003. Loss of bidirectional striatal synaptic plasticity in L-DOPA–induced dyskinesia. Nat. Neurosci. 501–506. https://doi.org/10.1038/nn1040

Pinault, D., 2008. N-methyl d-aspartate receptor antagonists ketamine and MK-801 induce wake-related aberrant gamma oscillations in the rat neocortex. Biol. Psychiatry 63, 730–5. https://doi.org/10.1016/j.biopsych.2007.10.006

Richter, U., Halje, P., Petersson, P., 2013. Mechanisms underlying cortical resonant states: implications for levodopa-induced dyskinesia. Rev. Neurosci. 24, 415–29. https://doi.org/10.1515/revneuro-2013-0018

Robelet, S., Melon, C., Guillet, B., Salin, P., Kerkerian-Le Goff, L., 2004. Chronic L-DOPA treatment increases extracellular glutamate levels and GLT1 expression in the basal ganglia in a rat model of Parkinson’s disease. Eur. J. Neurosci. 20, 1255–1266. https://doi.org/10.1111/j.1460-9568.2004.03591.x

Rothwell, P.E., Hayton, S.J., Sun, G.L., Fuccillo, M. V., Lim, B.K., Malenka, R.C., 2015. Input- and Output-Specific Regulation of Serial Order Performance by Corticostriatal Circuits. Neuron 88, 345–356. https://doi.org/10.1016/j.neuron.2015.09.035

Rubenstein, J.L.R., Merzenich, M.M., 2003. Model of autism: increased ratio of excitation/inhibition in key neural systems. Genes. Brain. Behav. 2, 255–267.

Shen, W., Flajolet, M., Greengard, P., Surmeier, D.J., 2008. Dichotomous dopaminergic control of striatal synaptic plasticity. Science (80-.). 321, 848–851. https://doi.org/10.1126/science.1160575

Sherman, S.J., Estevez, M., Magill, A.B., Falk, T., 2016. Case Reports Showing a Long-Term Effect of Subanesthetic Ketamine Infusion in Reducing L -DOPA-Induced Dyskinesias. Case Rep. Neurol. 8, 53–58. https://doi.org/10.1159/000444278

Tamte, M., Brys, I., Richter, U., Ivica, N., Halje, P., Petersson, P., 2016. Systems level neurophysiological state characteristics for drug evaluation in an animal model of levodopa-induced dyskinesia. J. Neurophysiol. jn.00868.2015. https://doi.org/10.1152/jn.00868.2015

Towers, S.K., Hestrin, S., 2008. D1-Like Dopamine Receptor Activation Modulates GABAergic Inhibition But Not Electrical Coupling between Neocortical Fast-Spiking Interneurons. J. Neurosci. 28, 2633–2641. https://doi.org/10.1523/JNEUROSCI.5079-07.2008

Voytek, B., Kramer, M.A., Case, J., Lepage, K.Q., Tempesta, Z.R., Knight, R.T., Gazzaley, A., 2015. Age-Related Changes in 1/f Neural Electrophysiological Noise. J. Neurosci. 35, 13257–65. https://doi.org/10.1523/JNEUROSCI.2332-14.2015

Whittington, M. a, Traub, R.D., Jefferys, J.G., 1995. Synchronized oscillations in interneuron networks driven by metabotropic glutamate receptor activation. Nature. https://doi.org/10.1038/373612a0

Williams, D., Tijssen, M., Van Bruggen, G., Bosch, A., Insola, A., Di Lazzaro, V., Mazzone, P., Oliviero, A., Quartarone, A., Speelman, H., Brown, P., 2002. Dopamine-dependent changes in the functional connectivity between basal ganglia and cerebral cortex in humans. Brain 125, 1558–1569. https://doi.org/10.1093/brain/awf156

Yang, C., Hu, Y.-M., Zhou, Z.-Q., Zhang, G.-F., Yang, J.-J., 2013. Acute administration of ketamine in rats increases hippocampal BDNF and mTOR levels during forced swimming

test. Ups. J. Med. Sci. 118, 3–8. https://doi.org/10.3109/03009734.2012.724118

Ye, T., Bartlett, M.J., Schmit, M.B., Sherman, S.J., Falk, T., Cowen, S.L., 2018. Ten-Hour Exposure to Low-Dose Ketamine Enhances Corticostriatal Cross-Frequency Coupling and Hippocampal Broad-Band Gamma Oscillations. Front. Neural Circuits 12, 61. https://doi.org/10.3389/fncir.2018.00061